Separation of colloidal nanoparticles using capillary immersion forces

Michael J Gordon, D. Peyrade

Separation of colloidal nanoparticles using capillary immersion forces

Michael J. Gordon[a] and David Peyrade[b]
Laboratoire des Technologies de la Microélectronique (LTM), CNRS, 17 Avenue des Martyrs, Grenoble 38054, France

(Received 10 April 2006; accepted 14 June 2006; published online 2 August 2006)

Capillary force assembly (CFA) of colloidal particles usually results in closed-packed films or particle aggregation within topographic features. In this work, it is shown that CFA can also be exploited to both localize and separate nanoparticles ($d=50-200$ nm) when template shape and wettability are controlled. Well-defined geometric arrangements of one to four closely spaced particles (30–50 nm separation) were realized in large arrays using this technique to demonstrate that particle aggregation during dewetting can be eliminated. Ordered SiO_2 nanopillars in tight groupings were obtained by combining low-resolution e-beam lithography (>100 nm) with CFA and etching. This approach provides a simple route to fast and precise placement of nanostructures using relatively low-resolution pattern making techniques. © *2006 American Institute of Physics*. [DOI: 10.1063/1.2266391]

Capillary forces have been used in a wide variety of experimental situations to assemble colloidal particles into periodic structures (colloidal crystals)[1–4] and filmlike nanocoatings[5] as well as to selectively deposit particles into topographic relief[6–11] or regions of enhanced wettability[11,12] on a solid surface. In these venues, capillary immersion forces[13] are ultimately responsible for arranging particles as the three-phase contact line of the colloidal solution moves across the surface (dewetting). When the liquid film entraining particles becomes thinner than the particle diameter (near the macroscopic contact line), the liquid meniscus around each particle gives rise to normal and lateral surface tension forces which can overcome Brownian motion.[13] Any constraint or process which modifies the liquid free surface near a particle (i.e., particle wettability,[13] evaporation,[14] contact line pinning,[15] etc.) can affect organization by modifying the strength and direction of the immersion force.

Capillary force assembly (CFA) requires that the substrate and particle surfaces be partially wettable; in this case, immersion forces are always attractive (particle-particle and particle-surface).[13] As a result, close-packing or particle aggregation within features and wettable regions commonly occurs (see Refs. 1–12). If the pattern or pinning site can accommodate more than one particle, immersion forces will group particles together when the particle loading is high. However, in this letter, we show that aggregation need not be the end result of CFA when relief patterns are considerably larger than the particle size. In fact, with proper pattern geometry and sufficient wettability contrast, immersion forces can be used to *separate* nanoparticles and to create organized groupings of two to four nontouching particles with spacings smaller than the particle diameter—without resorting to one particle per hole. Moreover, the ability to closely space particles offers additional freedom in pattern making at the nanoscale; for example, this "separation-based" CFA approach was used to create surface organization (i.e., high-density SiO_2 nanopillars) on a scale that is difficult using low-resolution lithography techniques.

Organization experiments were carried out using colloidal Au particles ($d=50-100$ nm, 10^9-10^{11} particles/ml, and citrate method[16]) and controlled dewetting where a patterned substrate was placed near vertical in a solution bath that was evaporating at a specified rate. Contact line velocities were varied from ~0.1 to 2 μm/s by restricting evaporation mechanically or by raising the bath temperature. Lithographic patterns consisted of a mix of micron-sized polygons, lines, and 50×50 arrays of holes (circles, rectangles, triangles, and squares) fabricated via e-beam (Leica VB6-HR). UV3 photoresist (Rohm & Haas), spin coated to 200–400 nm thickness on SiO_2/Si substrates, was the template. The resist/water contact angle before deposition was frequently adjusted with a short O_2 plasma treatment and the resist template after deposition was completely removable by plasma stripping without disturbing particle organization. Finally, patterns were transferred into the underlying SiO_2 layer using nanoparticles as a hard mask via reactive ion etching (CHF_3/O_2).

Figure 1(a) shows the common result of a reasonably well-tuned capillary force indexation process using 100 nm Au nanoparticles (NPs). Slow dewetting speed, ample particle concentration at the moving contact line, and large relief (350 nm depth) result in complete filling of the pattern with several NP layers. In contrast, Fig. 1(b) demonstrates what happens when pinning is strong and the evaporation rate is not uniform (and too fast) due to intermittent self-pinning[14] by NPs that overload the contact line region. The stick-slip or "wavelike" deposition within the pattern occurs because the intermittently pinned contact line acts as a particle sink[17,18] until the liquid meniscus suddenly springs back, leaving an empty zone behind.

When well-defined hole geometries are used [Fig. 1(c)], highly controlled pattern filling can be obtained, allowing one-, two-, three-, and four-particle groupings to be created. Certainly, the overall pattern size controls the number of particles deposited per hole in a global sense. However, the fact that nearly all holes (>80%, verified by dark-field spectroscopy on each hole) in the 50×50 array contain exactly the intended number of particles suggests that particle saturation at the contact line just balances the need for particles dictated by the hole shape, pattern density, and dewetting speed. In

[a]Electronic mail: gordonmi@chartreuse.cea.fr
[b]Electronic mail: david.peyrade@cea.fr

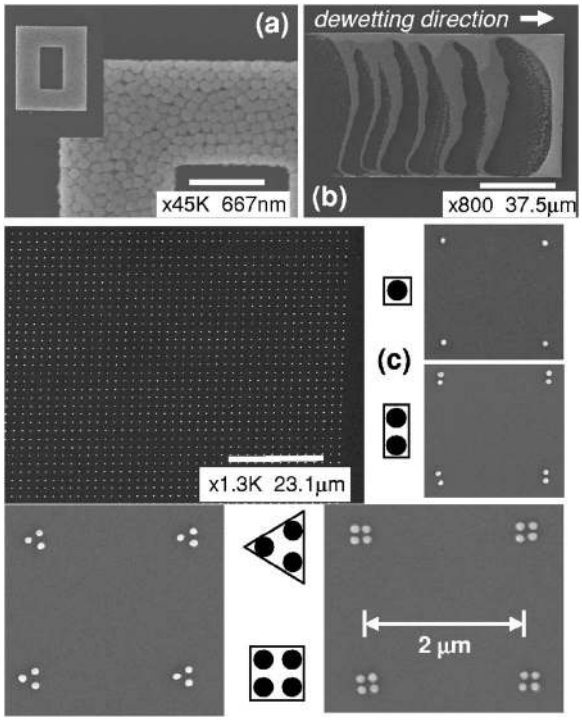

FIG. 1. Well-controlled (a) and haphazard (b) particle organization using 100 nm Au NPs and UV3 resist patterns (after template removal). (c) Highly controlled pattern filling can be achieved over very large areas of $100\times100\ \mu m^2$ and different hole geometries (as noted) allow one-, two-, three-, and four-particle groupings to be created.

other words, the contact line region must be "sufficiently" full of NPs—but not overloaded. For example, sporadic filling (more and less than dictated by geometry) due to self-pinning frequently occurred when the colloidal solution was too concentrated or when small aggregates at the contact line were dragged across the pattern (observed via real-time dark field during dewetting). Looking at the results of Fig. 1(c), one striking feature about organization is apparent: unlike most CFA processes, aggregation within the hole is never seen. This observation is quite surprising if we consider that in larger patterns with SiO_2 at the bottom [Fig. 1(b)], particles deposit individually or as aggregates where NPs are in intimate contact. For large patterns, the attractive immersion force (aided by convection[1,14]) drives aggregation when the liquid layer is thin. However, in smaller patterns where wall effects are not negligible, aggregation can be prevented under the right conditions. In this case, the role of immersion forces within the hole appears "reversed" from the normal outcome of CFA. Reasons for this stem from differences in wettability between the template material (upper surface and walls) and pattern bottom (SiO_2) as well as from meniscus asymmetry within the hole due to the hole geometry. Once in the hole, particles always prefer to migrate toward the corners or sharp regions of the pattern. For instance, the large square template in Figs. 2(a) and 2(c) was never filled with particles attaching to the edges of the square (i.e., 90° out from the orientation shown). Localization at the pattern corner is not counterintuitive when we consider that the liquid meniscus within the hole will likely have strong asymmetry towards the corner where two edges meet; however, it is not obvious how Young's criteria for the contact angle are maintained at the corner when the liquid droplet begins to be pinned by the hole. Setting this aside, it is clear that meniscus asymmetry at the corner functions as a particle sink. Furthermore, pattern filling was seen to be the most geometrically perfect, i.e., precise particle placement within the hole, for the triangle template where the corner angle was smallest (and presumably, meniscus distortion greatest).

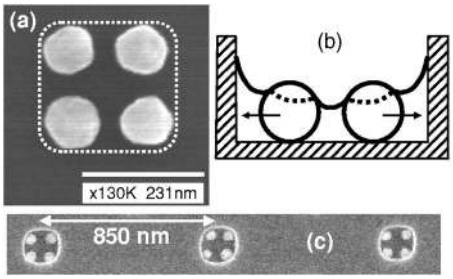

FIG. 2. (a) Isolated Au NPs (100 nm) after template removal (dashed square). (b) Probable free surface of the liquid in the pattern which leads to particle separation. The overall tilt of the particle contact line results in a net lateral force toward the wall and corners. (c) 50 nm Au NPs in the resist template, demonstrating particle preference for the pattern corners.

The fact that particles are separated during solvent evaporation within the hole indicates that the contact line around the particle has a net tilt toward the wall/corner [Fig. 2(b)]. Since particles do not show any chemical or charge-related affinity for the resist (i.e., there was no particle deposition between holes), particle attraction toward the corner area demonstrates that the separation process has physical origin—effectively controlled by liquid pinning at the template wall. Microscope studies of evaporating sessile drops of colloid on UV3 and SiO_2 show that the macroscopic contact angle and pinning on these surfaces are drastically different. For instance, the contact angle starts out at $\theta\sim55°-60°$ and must decrease to 30°–35° on UV3 before any contact line motion occurs (i.e., the droplet has a constant diameter with curvature radius increasing, until θ reaches $\sim30°$; then, the droplet shrinks in diameter). However, for SiO_2, θ begins near 40° and slowly decreases to $\sim15°-20°$ with the droplet diameter decreasing concomitantly. This disparity in contact angle between the template wall and bottom, as well as the increased "stickiness" of UV3, would certainly favor the situation depicted in Fig. 2(b). Thus, the pattern wall acts as an intermittent pinning site for the liquid nanodroplet forming in the hole when the contact line of the bulk solution pinches off from the hole. Such a pinned state would encourage particles to displace toward the walls. However, the fact that nearly every hole contains the desired number of particles (dictated by geometry) might suggest that the time scale for indexation is slow, compared to Brownian "stirring" of particles, so that localization toward the corner occurs on a particle-by-particle/corner-by-corner basis. In this case, a NP that has "already" been pulled to the corner may encourage further distortion of the liquid meniscus above/in the hole before final pinch off—making lateral immersion forces and the "particle sinking" effect of the remaining (unfilled) corners even stronger. Dark-field microscopy during evaporation confirms that particles can rearrange within a pattern after the main liquid front has detached from the pattern; necessarily then, a pinned liquid nanodroplet state should exist in the hole which allows some additional particle movement before all of the solvent evaporates.

Finally, as a proof of concept, nanoparticle groupings were used as an etching mask for pattern transfer into SiO_2

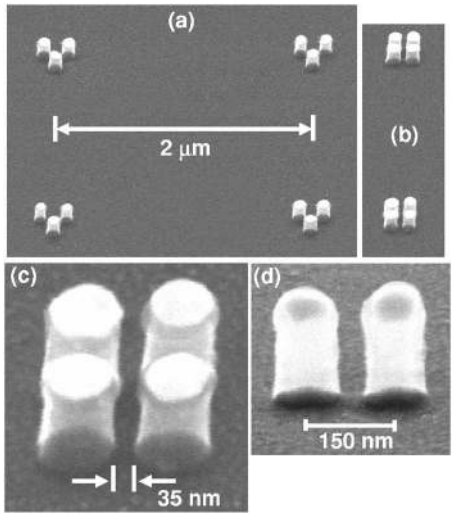

FIG. 3. [(a)–(d)] High-density pattern transfer into SiO_2 using Au NPs as a hard mask. Separation of NPs within the template due to immersion forces allows more freedom in surface nanostructuring. NP groupings are seen to be extremely robust despite resist stripping and reactive ion etching.

via reactive ion etching. For example, the NP patterns from Fig. 1(c) were used to fabricate SiO_2 pillars on Si where desired (Fig. 3) at high densities. Pattern replication was excellent and spacings could be varied from ~30 to 50 nm [Figs. 3(c) and 3(d)] for groupings of two to four posts by adjusting the template size. Overall, particle organization was seen to be exceptionally robust; resist stripping and etching did not disturb the NP placement.

In conclusion, we have demonstrated that particle aggregation during capillary force assembly processes can be prevented using lithographic features with proper geometric design and sufficient wettability contrast. In all localization experiments, we saw a strong preference for particles to migrate toward the corners of patterns. This organization scheme allowed closely spaced, nontouching particle groupings to be created at very high density—where desired. Thus, it is possible to combine indexation via CFA and controlled particle separation to create organized nanostructures at resolutions much smaller than that used in the lithography step which defines the template. In this way, the high-throughput aspect of low-resolution lithography can be directly extended down to length scales <100 nm.

[1] A. S. Dimitrov and K. Nagayama, Langmuir **12**, 1303 (1996).
[2] Q. H. Wei, D. M. Cupid, and X. L. Wu, Appl. Phys. Lett. **77**, 1641 (2000).
[3] D. K. Lee, E. M. Seo, and D. Y. Kim, Appl. Phys. Lett. **80**, 225 (2002).
[4] Y. H. Ye, S. Bedilescu, V. V. Truong, P. Rochon, and A. Natansohn, Appl. Phys. Lett. **79**, 872 (2001).
[5] B. G. Prevo and O. D. Velev, Langmuir **20**, 2099 (2004); B. G. Prevo, J. C. Fuller, and O. D. Velev, **17**, 28 (2005).
[6] Y. Yin, Y. Lu, and Y. Xia, J. Mater. Chem. **11**, 987 (2001); Y. Yin, Y. Lu, B. Gates, and Y. Xia, J. Am. Chem. Soc. **123**, 771 (2001).
[7] Y. Cui, M. T. Björk, J. A. Liddle, C. Sönnichsen, B. Boussert, and A. P. Alivisatos, Nano Lett. **4**, 1093 (2004).
[8] J. A. Liddle, Y. Cui, and P. Alivisatos, J. Vac. Sci. Technol. B **22**, 3409 (2004).
[9] M. Allard, E. H. Sargent, P. C. Lewis, and E. Kumacheva, Adv. Mater. (Weinheim, Ger.) **16**, 1360 (2004).
[10] T. Krauss, L. Malaquin, E. Delamarche, H. Schmid, N. D. Spencer, and H. Wolf, Adv. Mater. (Weinheim, Ger.) **17**, 2438 (2005).
[11] P. Maury, M. Escalante, D. N. Reinhoudt, and J. Huskens, Adv. Mater. (Weinheim, Ger.) **17**, 2718 (2005).
[12] F. Fan and K. J. Stebe, Langmuir **20**, 3062 (2004).
[13] P. A. Kralchevsky, V. N. Paunov, I. B. Ivanov, and K. Nagayama, J. Colloid Interface Sci. **151**, 79 (1992); P. A. Kralchevsky and K. Nagayama, Langmuir **10**, 23 (1994); P. A. Kralchevsky and N. D. Denkov, Curr. Opin. Colloid Interface Sci. **6**, 383 (2001).
[14] R. D. Deegan, Phys. Rev. E **61**, 475 (2000); R. D. Deegan, O. Bakajin, T. F. Dupont, G. Huber, S. R. Nagel, and T. A. Witten, *ibid.* **62**, 756 (2000).
[15] P. G. de Gennes, Rev. Mod. Phys. **57**, 827 (1995).
[16] Unconjuated gold colloids, British Bio-cell, Ltd.
[17] E. Adachi, A. S. Dimitrov, and K. Nagayama, Langmuir **11**, 1057 (1995).
[18] R. D. Deegan, O. Bakajin, T. F. Dupont, G. Huber, S. R. Nagel, and T. A. Witten, Nature (London) **389**, 827 (1997).